An investigation of anharmonic atomic vibrations of gamma -CuCl and gamma -CuBr by powder neutron diffraction

1994 J. Phys.: Condens. Matter 6 9949

(http://iopscience.iop.org/0953-8984/6/46/013)

J. Phys.: Condens. Matter 6 (1994) 9949–9962. Printed in the UK

An investigation of anharmonic atomic vibrations of γ-CuCl and γ-CuBr by powder neutron diffraction

F Altorfer†§, B Graneli‡, P Fischer† and W Bührer‡

† Laboratory for Neutron Scattering ETHZ & PSI, CH-5232 Villigen PSI, Switzerland

‡ Departement of Physics, Luleå University of Physics, S-971 87 Luleå, Sweden

Received 26 April 1994, in final form 2 September 1994

Abstract. Powder neutron diffraction measurements were made on CuCl and CuBr solid ion conductors over large ranges of temperature in the cubic γ phase (sphalerite structure). Anharmonic data treatment based on the Gram–Charlier expansion showed significant contributions up to fourth order for the thermal parameters of Cu. The thermal motion of Cu is strongly elongated along the tetrahedral diagonals. The corresponding probability density maps and the derived potential functions illustrate the characteristics.

1. Introduction

High ionic conductivity and large thermal vibrations are pronounced in 'true' ionic conductors, i.e. those having an enthalpy of migration about an order of magnitude larger than the thermal energy. They are not likely to be well described in the harmonic approximation, because of the relatively shallow potential wells for the migrating ions.

The cuprous halides provide attractive systems for the study of anharmonic effects, structural phase transitions and superionic conductivity. In the low-temperature γ phase CuCl and CuBr crystallize in the sphalerite structure (space group $F\bar{4}3m$) with Cu and Cl (Br) on sites 4c $(\frac{1}{4}, \frac{1}{4}, \frac{1}{4})$ and 4a $(0, 0, 0)$, respectively. CuBr (CuCl) undergoes at $T_{\gamma\rightarrow\beta} = 658$ K (680 K) a structural phase transition into a hexagonal phase (β, wurtzite) [1]. CuBr shows at $T_{\beta\rightarrow\alpha} = 743$ K a second solid–solid transition into a cubic (α) modification where the Cu ions are highly disordered, a behaviour similar to the excellent ionic conductor AgI with $T_{\beta\rightarrow\alpha} = 419$ K. CuCl does not possess a cubic α phase at normal pressure but melts at 696 K. The temperature dependence of the ionic conductivity of CuCl and CuBr shows a strong increase on approaching the γ–β transition, followed by a further moderate increase in the β phase up to the transition into the superionic conducting α phase (CuBr) or the liquid (CuCl) [2].

Structural as well as lattice dynamical investigations of the γ phase of cuprous halides showed as functions of the temperature large and unexpected effects: (i) CuCl has a negative thermal expansion at low temperature [3]; (ii) in inelastic neutron scattering experiments, CuCl and CuBr show strongly damped one-phonon maxima even at liquid nitrogen temperature [4, 5]; (iii) copper ions in CuBr and CuCl perform very large thermal motion: root mean square displacements below the $\gamma \rightarrow \beta$ (solid–solid) phase transition are comparable to values of normal ionic solids close to the melting point.

§ Present address: Reactor Radiation Division, National Institute of Standards and Technology, Gaithersburg, MD-20899, USA.

0953-8984/94/469949+14$19.50

In the harmonic approximation thermal vibrations of atoms are constrained such that the time averaged probability function for the position is a Gaussian function of the displacements from the equilibrium position, leading to spherical contours of equal probability for the cuprous halides. However the point symmetry is tetrahedral ($\bar{4}3m$) for both ions, and at higher temperatures it can be expected that an ion spends more time along directions away from the nearest neighbours than towards them, resulting in a tetrahedral lobe contour for the averaged probability function. This anharmonic contribution will contribute to diffracted Bragg intensities, showing up in a careful measurement.

For the analysis of the experimental data there are basically two paths to follow: (i) models where the tetrahedral lobes are built up by a number of non-regular sites for the mobile ions with a simple approximation for the thermal parameters ('split site' models) or (ii) models expressing the distribution in terms of regular sites and highly anharmonic temperature factors. As long as little is known about the time of occupancy or about ionic diffusion paths both approaches might give reasonable results.

Favourite systems to study are those with known transitions to disordered states, but also the site symmetry of the involved ions has to be sufficiently high in order to keep the number of anharmonic parameters low. Detailed anharmonic investigations, i.e. data collection and analysis as a function of the temperature, have been performed for the fluorites BaF_2 [6] and SrF_2 [7], both systems with a Faraday type phase transition leading to anion disorder. To a lesser extent, i.e. data treatment at only one temperature and/or the split site model, the sphalerites ZnSe and ZnTe [8], CuBr [9, 10], CuCl [11, 12] and CuI [9, 13] have been studied.

In the present paper we report on an anharmonic analysis of neutron diffraction experiments on γ-CuCl and γ-CuBr powder samples in order to prove that powder measurements may lead to significant results with respect to anharmonicity. From the determined anharmonic parameters the probability density functions and the effective single-particle potentials are calculated, demonstrating the deviation from the low-temperature harmonic behaviour and giving information about barrier heights between lattice sites and possible diffusion paths.

2. Experimental details

Neutron powder diagrams of polycrystalline γ-CuBr and γ-CuCl were recorded with the multicounter diffractometer DMC [14] at the Saphir reactor (Paul Scherrer Institute, Würenlingen). The instrument simultaneously covers a scattering angle range of 80°. A primary collimator of 10′ may be inserted (in pile), leading to a so called 'high-resolution' mode of operation, so as to compare to the 'high-intensity' mode without primary collimation.

Commercially available CuBr (> 99% pure) was used for the diffraction experiments. Measurements were performed with a wavelength of the incoming neutrons of 1.701 Å in the 'high-resolution mode' configuration. The sample was encapsulated into a Cu container in order to ensure that the thermal gradients in the sample were small. Diagrams were recorded at T = 293 K, 383 K, 443 K, 508 K, 548 K and 623 K in a small furnace of the 'hot-finger' principle. At low temperature (35 K) a closed cycle He refrigerator was used ('cold finger'). The copper peaks from the container are on one hand disadvantageous (leading to excluded regions in the data treatment), but on the other hand are useful for wavelength calibration and checks of sample temperature.

CuCl was measured with a wavelength of the incoming neutrons of 1.190 Å at temperatures of 8 K, 151 K, 295 K, 373 K, 473 K and 633 K; the details of the experiment are given in [12].

Examples of measured diagrams are displayed in figure 1: (a) CuCl at 633 K and (b) CuBr at 538 K. The very strong Debye–Waller factor is noticeable, drastically reducing the scattered intensity at high 2Θ angles (and consequently also limiting the number of

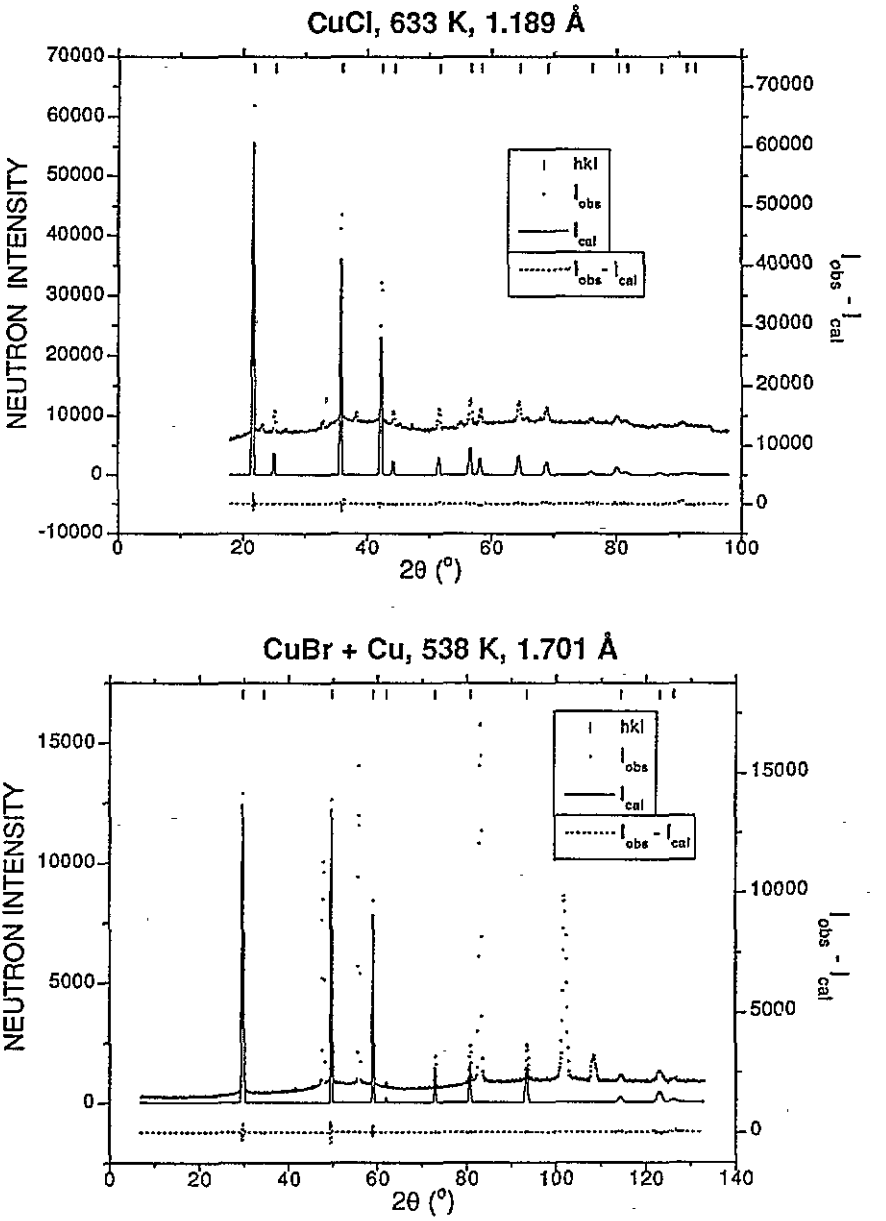

Figure 1. Observed, calculated (background subtracted) and difference neutron diffraction patterns; fourth-order anharmonic model with parameters given in table 1 (bold). (a) γ-CuCl at $T = 633$ K; (b) γ-CuBr at $T = 538$ K.

observable (hkl) reflections to ~ 16), and the strong modulated background due to phonon induced diffuse scattering. The very small foreign peaks in the CuCl data at 633 K originate most probably from the thermocouples.

The observed neutron intensities were corrected for absorption according to the measured transmission. The background (i.e. mostly incoherent scattering from sample, container and furnace), to be subtracted from the measured intensities, was approximated by consecutive straight lines. The influence of thermal diffuse scattering, for which no straightforward procedure for powder experiments is available at present, was not corrected in the raw data.

3. Theory

In elastic neutron scattering experiments (for an introduction see [15]) the Bragg intensities are proportional to

$$S(h) \approx \left| \sum_{\kappa=1}^{n} b_\kappa T_\kappa \exp[2\pi i \boldsymbol{h} \cdot \boldsymbol{r}_\kappa] \right|^2 \tag{1}$$

where $\boldsymbol{h}$ is a reciprocal lattice vector, b_κ is the coherent scattering length, and the summation is over all atoms at positions $\boldsymbol{r}_\kappa$ in the unit cell. The temperature factor T_κ accounting for the thermal motion of the atoms is the quantity of interest in the present context. Closely related to the temperature factor is the probability density function (PDF) of an atom. The PDF is the probability of finding an atom in the volume element d^3u when it is displaced by $\boldsymbol{u}$ from its average equilibrium position; it is given by the Fourier transform of the temperature factor [16]

$$p_\kappa(\boldsymbol{u}) = \frac{1}{(2\pi)^3} \iiint T_\kappa(\boldsymbol{Q}) \exp[-i\boldsymbol{Q} \cdot \boldsymbol{u}] \, d^3u \tag{2}$$

where $\boldsymbol{Q}$ is the scattering vector and

$$\int p_\kappa(\boldsymbol{u}) \, d^3u = 1. \tag{3}$$

The relation between the PDF and the effective one-particle potential $V(\boldsymbol{u})$ is given by [17]

$$p(\boldsymbol{u}) = (1/Z) \exp[-V(\boldsymbol{u})/(k_B T)] \tag{4}$$

with k_B = Boltzmann's constant and

$$Z = \iiint \exp[-V(\boldsymbol{u})/(k_B T)] \, d^3u. \tag{5}$$

Z can be calculated, if the energy at the equilibrium position of an atom is set to zero, and for the potential one obtains [18]

$$V(\boldsymbol{u}) = -k_B T \ln[p(\boldsymbol{u})/p(\boldsymbol{u} = 0)]. \tag{6}$$

In terms of the potential $V(\boldsymbol{u})$ of the crystal, the harmonic approximation stops the expansion with respect to the atomic displacements after the quadratic term, and the atomic vibrations can be described by harmonic oscillators. The PDF has the shape of a Gaussian and the

contours of equal probability are in general ellipsoids, but degenerate (by symmetry) to spheres for both atoms in the sphalerite structure, and therefore the temperature factor can be written as

$$T_\kappa^{\text{harm}}(Q) = \exp[-\tfrac{1}{2}Q^2\langle u(\kappa)^2\rangle] \tag{7}$$

where $\langle u(\kappa)^2\rangle$ is the mean square displacement of atom κ in any direction. It is related to the 'standard' isotropic temperature factors by

$$B_\kappa = 4\beta_\kappa a^2 = 8\pi^2\langle u(\kappa)^2\rangle \tag{8}$$

where a is the lattice constant.

In principle the harmonic model can be extended to include anharmonicity by a series expansion of either the temperature factor T_κ, the probability density PDF, or the potential $V(u)$. We follow the procedure given by Zucker and Schulz [18] with the expansion of the temperature factor in a Gram–Charlier series. The temperature factor up to fourth order is then given by

$$T_\kappa(h) = T_\kappa^{\text{harm}}(h)[1 + [(2\pi\mathrm{i})^3/3!]c_{pqr}h_ph_qh_r + [(2\pi\mathrm{i})^4/4!]d_{qprs}h_ph_qh_rh_s]. \tag{9}$$

In the sphalerite structure, symmetry strongly reduces the number of anharmonic coefficients and there are only one third-order (c_{123}) and two fourth-order (d_{1111}, d_{1122}) parameters per atomic site.

4. Results and discussion

Data analysis was performed with profile fitting routines based on the Rietveld method [19] for both the harmonic and the anharmonic models [20, 21], the latter making use of the Gram–Charlier expansion of the temperature factor. The coherent neutron scattering lengths were taken from Sears [22]. The method we followed in the refinement was to start with the low-temperature data and the harmonic model, and then extend the analysis to higher temperatures. In the minimization process we not only took care of the agreement factors but also of the parameter values, trying to restrict them to values within physical limits. In order to do this a step by step introduction of anharmonic parameters was necessary.

4.1. Harmonic model

The high (cubic) symmetry of the Cu and halogen sites (X = Cl, Br) restricts the thermal motion to be isotropic. In the harmonic model we have a total of eight parameters to refine: three quantities related to the structure of the sample (lattice constant and isotropic temperature factors of Cu and halogen), and five quantities related to the experiment (scale factor, three resolution parameters, the zero point of 2Θ, and a low-angle asymmetry parameter). The structural parameters of γ-CuCl and γ-CuBr are summarized in tables 1 and 2, respectively, together with the agreement factors for the profile, the nuclear structure factors (integrated intensities) and the expected factor (given by the counting statistics). The values of the harmonic model are given in the top line for each temperature. This model gives satisfactory factors of agreement for the lowest temperatures, rather good estimates of the isotropic thermal vibration parameters and good estimates of the lattice constants at all temperatures.

Table 1. Structural parameters of γ-CuCl, space group $F\bar{4}3m$, atomic positions 4c and 4a for Cu and Cl, respectively; R_{wp} and R_I are agreement factors concerning weighted profile and integrated intensities, respectively; R_{exp} is the expected value for the profile [19, 21]; standard deviations of parameters are given within parentheses and refer to the last digit.

T (K)	a (Å)	β (10^4) Cu	β (10^4) Cl	c_{123} (10^{-6}) Cu	d_{1122} (10^{-7}) Cu	R factors (%) R_{wp}	R_I	R_{exp}
8	5.4017(2)	8(5)	24(4)	—	—	7.7	2.4	4.0
		9(5)	23(4)	−2(1)	—	7.6	2.5	
		9(6)	**23(4)**	**−2(1)**	**0(1)**	7.6	2.5	
151	5.3994(2)	138(5)	93(3)	—	—	9.0	3.5	5.3
		138(5)	93(3)	1(3)	—	9.0	3.5	
		151(8)	**94(3)**	**1(3)**	**4(2)**	8.9	3.6	
295	5.4068(3)	342(10)	173(4)	—	—	11 4	5.8	7.1
		343(10)	174(4)	18(7)	—	11.3	5.6	
		380(17)	**178(4)**	**24(8)**	**18(8)**	11.2	5.4	
373	5.4169(2)	511(7)	219(2)	—	—	6.8	5.0	3.7
		514(6)	221(2)	40(5)	—	6.4	4.2	
		568(12)	**226(2)**	**53(6)**	**36(7)**	6.2	3.6	
473	5.4273(3)	687(9)	263(3)	—	—	7.3	5.3	3.4
		696(8)	267(3)	64(7)	—	6.8	4.6	
		757(15)	**272(3)**	**80(9)**	**52(11)**	6.6	4.0	
633	5.4568(4)	1034(9)	323(5)	—	—	7.6	5.7	2.8
		1065(17)	341(5)	160(18)	—	6.5	4.8	
		1117(28)	**344(5)**	**173(19)**	**62(28)**	6.5	4.6	

Table 2. Structural parameters of γ-CuBr; details are as for table 1.

T (K)	a (Å)	β (10^4) Cu	β (10^4) Cl	c_{123} (10^{-6}) Cu	d_{1122} (10^{-7}) Cu	R factors (%) R_{wp}	R_I	R_{exp}
35	5.6773(2)	34(6)	46(8)	—	—	7.8	2.0	2.4
		41(8)	46(9)	12(5)	—	7.7	1.6	
		80(19)	**48(8)**	**12(5)**	**13(6)**	**7.6**	**1.1**	
293	5.6897(3)	273(12)	144(8)	—	—	6.7	2.2	4.8
		263(16)	160(12)	24(5)	—	6.3	1.7	
		295(27)	**171(23)**	**29(6)**	**18(6)**	**6.1**	**1.0**	
383	5.6991(3)	412(10)	177(5)	—	—	6.3	2.6	4.0
		403(10)	187(5)	33(5)	—	5.8	1.6	
		438(18)	**191(6)**	**38(6)**	**18(7)**	**5.7**	**0.9**	
443	5.7072(3)	519(13)	220(5)	—	—	6.8	2.6	3.9
		514(13)	229(5)	49(7)	—	6.1	1.3	
		561(22)	**234(6)**	**60(8)**	**27(9)**	**5.9**	**0.7**	
508	5.7159(4)	626(16)	255(5)	—	—	7.0	3.3	3.8
		630(13)	263(5)	77(7)	—	5.5	1.3	
		693(22)	**271(5)**	**98(10)**	**40(11)**	**5.2**	**0.8**	
538	5.7192(3)	709(19)	276(6)	—	—	7.6	4.1	4.0
		724(15)	283(5)	99(9)	—	5.8	1.5	
		763(25)	**287(5)**	**112(12)**	**26(13)**	**5.8**	**1.4**	
622	5.7410(10)	920(49)	324(14)	—	—	16.4	6.5	7.8
		959(48)	338(14)	165(32)	—	15.3	3.4	
		989(78)	**337(15)**	**172(41)**	**27(5)**	**15.3**	**3.3**	

Experimental intensities have not been corrected for thermal diffuse scattering (TDS). It is shown by Cooper and Rouse in [23] that TDS in a fairly good approximation gives rise to a negative contribution $-\Delta\bar{B}$ to the mean temperature factor $\bar{B}$. The correction $\Delta\bar{B}$ is proportional to the temperature, to a function κ determined by the elastic constants c_{11}, c_{12} and c_{44} and to the instrumental resolution. Calculations of $\Delta\bar{B}$ yield for ZnS at 295 K ~ 0.04 Å^2 [8], and for BaF_2 at 700 K ~ 0.16 Å^2 [23]. Inserting the elastic constants of CuCl [4] and CuBr [5] into the expression for κ ([23], equations (3) and (4)) leads to similar values as for ZnS and BaF_2, and hence we estimate the TDS corrections to be of the same order. Compared to the absolute values of the mean temperature factors $\bar{B}$ of ~ 3 Å^2 for CuCl at 295 K ($\bar{\beta}$ from table 1, and (8)), the estimated TDS corrections are rather small and are therefore neglected.

The smallness of the estimated TDS around the Bragg positions is, in relation to the large $\bar{B}$ values and the strong background modulation in the diffraction patterns at elevated temperatures, not contradictory: it can be explained by the rather unusual lattice dynamics of CuCl and CuBr [4, 5]. Both compounds have very flat and energetically low-lying phonon branches (below 5 meV), which are thermal easily activated. Furthermore the flat regions extend over large parts of the Brillouin zone, resulting in large weights in the summation over all phonon modes for the determination of the mean square displacements $\langle u(\kappa)^2\rangle$ and of the phonon induced diffuse scattering [16]. As compared to a normal ionic solid (e.g. NaCl), in CuX the above mentioned lattice thermal properties are strongly determined by non-zone centre phonon modes, giving rise to considerable effects in extended regions of reciprocal space (and not only near Bragg positions where elastic constants give a good estimate of phonon contributions).

4.2. Quasiharmonic model

Quasiharmonic behaviour as the simplest approximation to the effects on heating is discussed by Willis and Pryor [16]. The relative change in volume $\delta v/v$ due to expansion gives a relative frequency change $\delta\omega/\omega$ of atomic vibrations

$$\delta\omega/\omega = -\gamma_G \delta v/v = -\gamma_G \chi T \tag{10}$$

where γ_G is the Grüneisen constant and χ the volume coefficient of expansion. The softening of the vibrational frequencies gives rise to an increase of the thermal motion, which for the isotropic case results in a change of the temperature factor

$$B = B^h(1 + 2\gamma_G \chi T) \tag{11}$$

where h refers to the harmonic value. In order to consider quasiharmonic effects, harmonic data as well as Grüneisen constants have to be known. Detailed γ_G values are not available for the cuprous halides, but information on the product $\gamma_G\chi$ may be obtained from coherent inelastic neutron scattering. Measurements of phonon dispersion curves give for CuCl an average frequency change of -0.06 between 4 K and 295 K [4], and approximately the same value can be estimated for CuBr between 77 K and 295 K [5]. Harmonic values of mean square displacements result from model calculations of eigenvector weighted density of states; values as a function of the temperature are given in figure 2(a) for CuCl [4] and (b) for CuBr [5]. Derived quasiharmonic values are also displayed; for CuCl the onset of quasiharmonicity has been set at $\sim$ 100 K, the temperature where the initially negative thermal expansion turns to a normal positive value. As compared to our experimental points, the estimated quasiharmonic data look reasonable for Cu but neither for Cl nor for Br,

because at all temperatures the calculated harmonic values are larger than the corresponding experiments. These experimentally determined β_X parameters for Cl and Br are however well defined and model independent (subsection 4.3, tables 1 and 2), they show a linear behaviour as a function of the temperature and tend to zero for 0 K (excluding static defect contributions); TDS corrections are not that important, and therefore one has to try to account for the systematic difference with respect to the calculation.

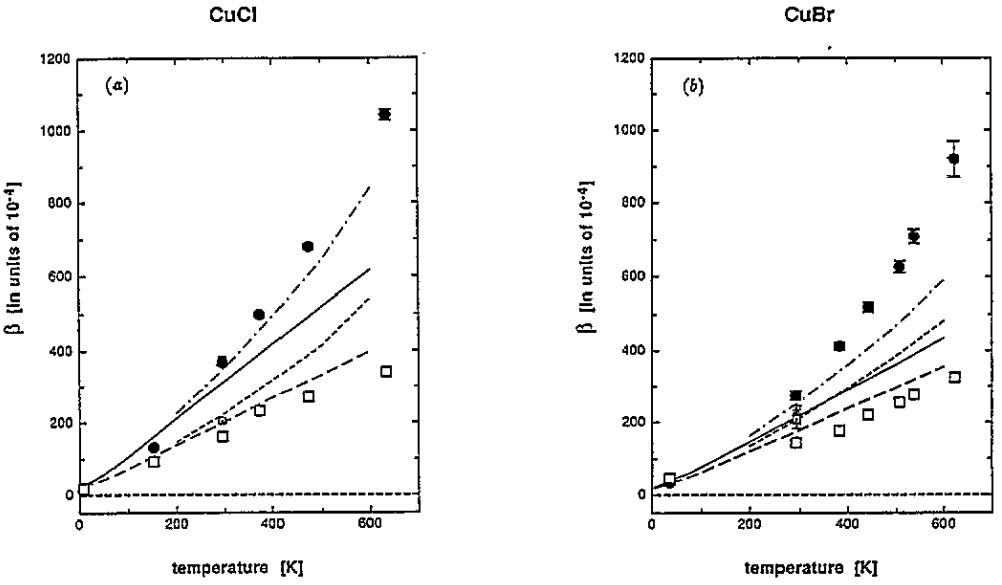

Figure 2. The temperature dependence of the thermal parameters β_{Cu}, β_X, X = Cl, Br. Experimental points as obtained from harmonic fit (table 1): ●, Cu; □, X. Harmonic lattice dynamical calculation: ——, Cu; – – –, X. Quasiharmonic corrections: — · —, Cu; ----, X. (Both as discussed in the text.) (a) γ-CuCl (⊙, Cu; ⊡, Cl [11]); (b) γ-CuBr, (⊙, Cu; ⊡, Br [25]).

Lattice dynamical models are generally established by fitting parameters to measured phonon frequencies (eigenvalues of the dynamical matrix) and not to one-phonon intensities (determined by the eigenvectors of the dynamical matrix), and hence there remains some arbitrariness in the type as well as in the values of model parameters. Hoshino *et al* [5] indeed present two different parameter sets of the shell model with almost equally good fits to the phonon frequencies. Subsequent calculations however show rather different eigenvectors leading to very different mean square atomic displacements. Their choice of the 'more physical' parameter set was finally based on a comparison with mean square displacements from x-ray diffraction experiments. In other words, although lattice dynamical calculations are performed in the harmonic approximations, derived results can be far away from real harmonic values, and only a self-consistent treatment of lattice dynamical and diffraction data as a function of the temperature would result in reliable harmonic values.

Having the arbitrariness of model calculations in mind, we feel confident that our experimental points and their almost linear dependence on temperature represent adequate harmonic thermal motions of Cl and Br in cuprous halides. By subsequently applying quasiharmonic corrections the use of an overall Grüneisen constant is not appropriate in

order to describe the different temperature dependence of Cu and halogen ions; better results might be obtainable by using mode and temperature dependent Grüneisen constants, which however are not known. The (formal straightforward) quasiharmonic approximation cannot therefore be reliably performed for the cuprous halides.

4.3. Anharmonic models

Third-order anharmonic temperature factors for interpreting neutron diffraction data of the sphalerite structure have been discussed by Cooper *et al* [8]. In the harmonic approximation there are three types of structure factor for reflections with $h+k+l = 4n$, $h+k+l = 4n+2$ and $h+k+l =$ odd, respectively. Taking into account third-order anharmonic contributions leads to a split of the odd reflections into $h+k+l = 4n \pm 1$, and exactly these reflections are significantly sensitive to third-order anharmonic contributions. The number of third-order parameters is restricted by symmetry to only one for Cu and halogen; however as pointed out by Cooper *et al* [8] these parameters appear as weighted difference in the structure factor and cannot individually be determined, the respective weights being proportional to $(\beta_{Cu})^3$ and $(\beta_X)^3$. By inserting the fitted β_i values of tables 1 and 2, we can estimate that already at room temperature the weight of the third-order halogen parameter in CuBr (CuCl) is about a factor of seven (12) smaller than the weight of the third-order copper parameter. Therefore in the subsequent calculations the halogen third-order parameter was set equal to zero.

Results of the refinements are summarized in tables 1 and 2 for CuCl and CuBr, respectively. As compared to the harmonic model, agreement factors improve significantly for temperatures higher than 295 K. The introduction of the third-order parameter c_{123} for Cu does not considerably change the values of the harmonic parameters β_i of Cu and halogen, a hint at the stability and physical significance of these second-order (harmonic) contributions.

A next step is then to consider the fourth-order terms. Symmetry restricts the number of these parameters to two, an isotropic and an anisotropic term (d_{1111} and d_{1122} in the notation of Zucker and Schulz [18]). Cu and halogen ion sites both allow for fourth-order terms, but we restrict our analysis to the Cu part for the following reasons: (i) ionic conductivity proves Cu to be the mobile ion and hence it should have a shallower potential and (ii) the introduction of additional parameters (series expansion of the temperature factor) is only meaningful if those already in use, i.e. second and third order, do not change considerably, thus giving a cross-check of the expansion and fitting procedure. The isotropic fourth-order term has the same symmetry as the second-order term, and hence on one hand ideally can give a correction to the potential, but on the other hand is strongly correlated to the second-order term, and as discussed by Mair *et al* [7] both parameters cannot be refined simultaneously. A way to overcome this problem is to fix the second-order term to the quasiharmonic value, and then to refine only the fourth-order term. However as shown in the previous section quasiharmonic values cannot reliably be obtained, and therefore we set $d_{1111} = 0$ for the analysis.

Results of the refinements are given in tables 1 and 2 for CuCl and CuBr, respectively (bottom lines at each temperature, bold). As compared to the third-order anharmonic model, agreement factors are improving, and in particular more significantly for R_I than for R_{wp} as discussed in detail by Boysen [21], leading to satisfactory values for all temperatures; furthermore the introduction of the fourth-order parameter significantly influences neither the second-order nor the third-order parameters. The corresponding calculated neutron diffraction patterns of CuCl at 633 K and CuBr at 538 K are shown in figure 1(a) and (b), respectively.

The temperature dependence of the thermal parameters β_{Cu}, β_X, c_{123}^{Cu} and d_{1122}^{Cu} is displayed in figure 3(a) and (b) for CuCl and CuBr, respectively. As a function of the temperature a systematic behaviour of all the thermal parameters can be observed: a roughly speaking quadratically increasing β_{Cu}, a lincarly increasing β_X, a rather well defined and quadratically increasing c_{123}^{Cu} (larger in CuCl than in CuBr), and a small not very well determined d_{1122}^{Cu}. Noticeable (tables 1 and 2) is the fact that the second-order parameters β_X of Cl as well as of Br are really almost model independent within the rather small error limits, thus supporting our discussion on harmonic model calculations.

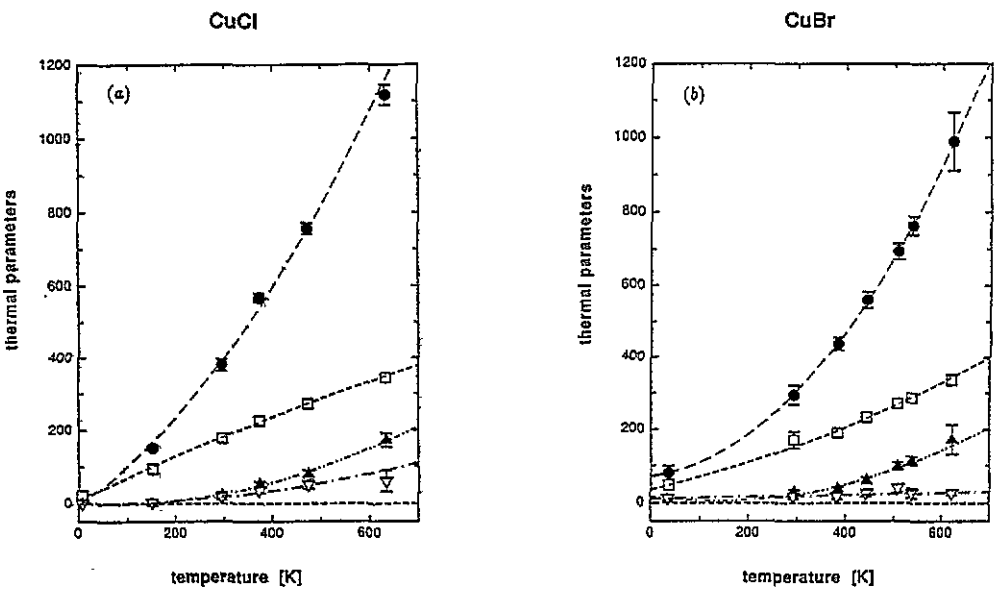

Figure 3. The temperature dependence of the thermal parameters β_{Cu}, β_X, c_{123}^{Cu} and d_{1122}^{Cu} of γ-CuBr and γ-CuCl, as obtained from the anharmonic fits (fourth order) (tables 1 and 2); β_{Cu}, β_X are in units of 10^{-4}, c_{123}^{Cu} is in units of 10^{-6} and d_{1122}^{Cu} is in units of 10^{-7}; the lines are fitted parabolic curves to guide the eye. (a) γ-CuCl: ●, β_{Cu}; □, β_{Cl}; ▲, c_{123}^{Cu}; ▽, d_{1122}^{Cu}. (b) γ-CuBr: ●, β_{Cu}; □, β_{Br}; ▲, c_{123}^{Cu}; ▽, d_{1122}^{Cu}.

Parameters resulting from the refinement (tables 1 and 2) have been used to calculate the PDF distributions. As examples, the maps of Cu in CuX for different temperatures and models are displayed in figures 4. CuCl at 633 K is shown as follows: (a) harmonic model, (b) with third order c_{123}^{Cu} and (c) with third and fourth order d_{1122}^{Cu}. The third-order parameter creates not only a strong deviation from the spherical contour but in addition sharpens the PDF in the centre. The fourth-order parameter corrects this effect in the centre (i.e. back to the harmonic, broad contour), but furthermore flattens the PDF perpendicular to [001]. CuCl at 373 K for the fourth-order anharmonic model is shown in (d); the above mentioned features are already present but the distribution is less extended in space. The corresponding PDF maps for Cu in CuBr at 538 K are shown in figure 4(e) for the harmonic model and figure 4(f) for the fourth-order anharmonic model; the same asymmetry as in CuCl is observed, but its magnitude is smaller, similar to e.g. Cu in CuCl at 473 K. Regions of negative (unphysical) values of the PDF distributions (marked in light grey) are very weak; the absolute values of the minima are less than 1% of the maxima (i.e. less than 10% of

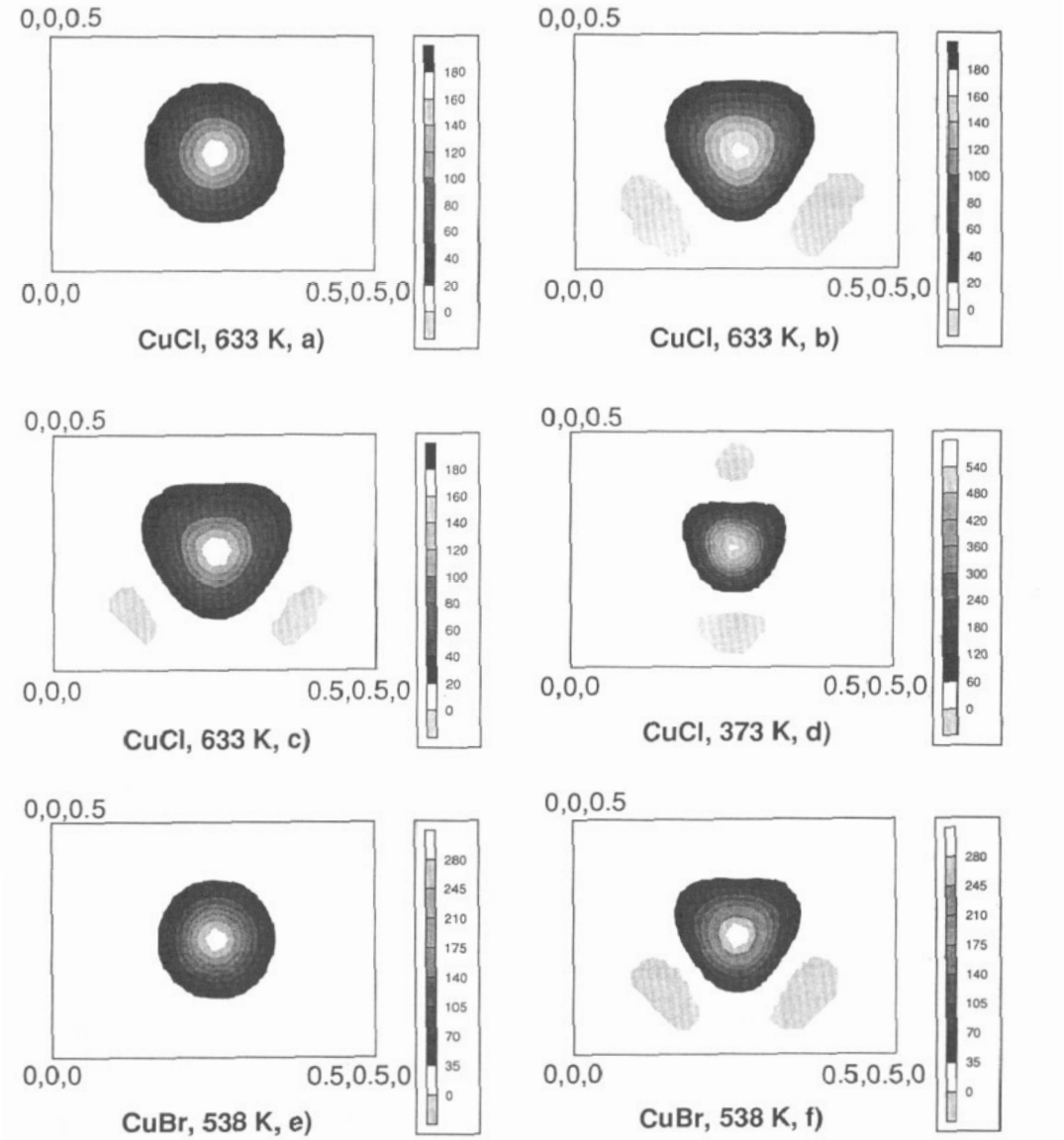

Figure 4. PDF maps of Cu in CuX in the $(1\bar{1}0)$ plane, as derived from the model parameters (tables 1 and 2), scale factor 100: (a) γ-CuCl at 633 K, harmonic model, $I_{max} = 174$; (b) γ-CuCl at 633 K, third-order anharmonic model, $I_{max} = 166$, $I_{min} = -2$; (c) γ-CuCl at 633 K, fourth-order anharmonic model, $I_{max} = 177$, $I_{min} = -1$; (d) γ-CuCl at 373 K, fourth-order anharmonic model, $I_{max} = 563$, $I_{min} = -3$; (e) γ-CuBr at 538 K, harmonic model, $I_{max} = 305$; (f) γ-CuBr at 538 K, fourth-order anharmonic model, $I_{max} = 309$, $I_{min} = -4$.

a contour step along the positive direction) and can therefore be considered as artefacts of the calculation. The computed PDF maps give evidence that the higher-order thermal coefficients are not fitting parameters for minimizing the factors of agreement but represent a physically meaningful behaviour.

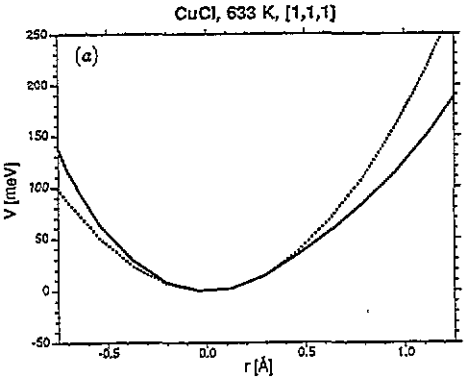

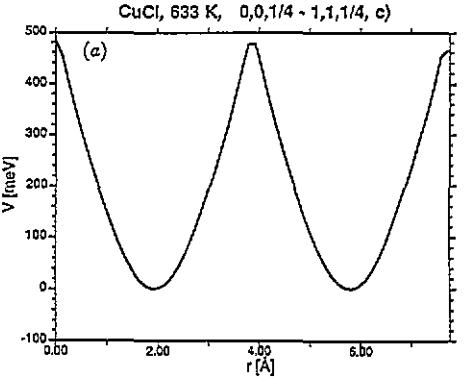

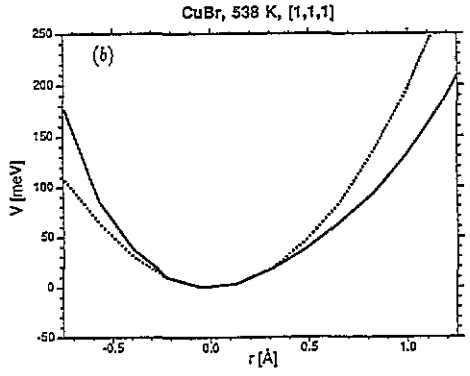

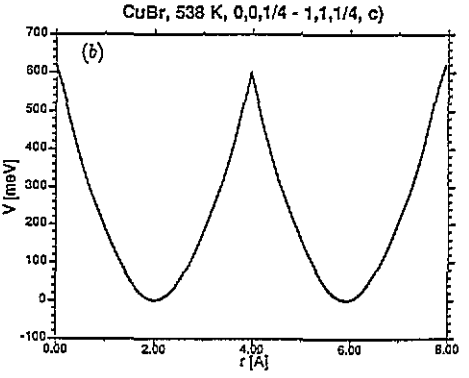

Figure 5. The Cu potential in CuX along the [111] direction for different models: ·····, harmonic; ——, fourth-order anharmonic. (a) γ-CuCl at 633 K; (b) γ-CuBr at 538 K.

Figure 6. The Cu potential in CuX along the [110] direction calculated with the fourth-order model; (a) γ-CuCl at 633 K; (b) γ-CuBr at 538 K.

Corresponding calculated potential distributions for Cu are shown in figure 5(a) for CuCl at 633 K and (b) for CuBr at 538 K. The asymmetry created by c_{123}^{Cu} is very pronounced along the [111] direction with the hardening towards the neighbouring halogen and the softening towards the empty site $(\frac{1}{2}, \frac{1}{2}, \frac{1}{2})$. The calculated potentials along [110] are displayed in figure 6(a) for CuCl at 633 K and (b) for CuBr at 538 K. The potential height is estimated to be 0.60 eV (0.48 eV) for CuBr (CuCl). If we interpret the ionic conduction mechanism by thermally induced Frenkel defects and a hopping process of Cu by way of regular lattice sites, it is this potential barrier which determines the parameters of an Arrhenius law. The calculated result however cannot quantitatively be compared with experimental data for the following reasons: (i) measurements on tracer diffusion and ionic conductivity of Cu in CuBr [24] showed deviations from an Arrhenius behaviour and (ii) the diffusion coefficient of the tracer experiment turned out to be considerably larger than the value of the conductivity experiment. Therefore for the diffusion of Cu in CuBr, instead of a simple one-step process, a diffusion mechanism built up by several steps, and with at least one strong component not contributing to the net charge transport, was suggested. Average values of activation energies for temperatures around 530 K can be estimated to be 1.05 eV and 1.26 eV for tracer and conductivity experiments, respectively. The tracer value of the

activation energy is larger than our calculated potential barrier and hence the jump frequency is smaller, a behaviour that can be qualitatively understood because correlations (the back-jump probability of an ion) as well as the 'site blocking factor' (not many unoccupied sites for the realization of a jump) will give a reduction of the number of jumps leading to long-range transport.

5. Conclusions

Powder neutron diffraction data of CuX (X = Cl, Br) were analysed in large temperature ranges with anharmonic models up to fourth order. On the one hand the information to be obtained from experiments on powders, as compared to single-crystal experiments, is limited because the number of observable reflections is lower and furthermore peaks might overlap, but on the other hand data corrections such as extinction and absorption are easier to handle. Nevertheless the relatively small number of observations might give restrictions with respect to the number of anharmonic parameters to be determined in the refinement process. The γ phases of CuCl and CuBr are in this respect very favourable systems: the structure is FCC and the site symmetry is high, and as a consequence there are no free positional parameters of the atoms and the number of anharmonic parameters is small. Therefore reliable values of the parameters can be determined despite the limited number of observations.

In order to obtain insight into the anharmonic behaviour and to check the physical significance of the fitted parameters it is important to perform experiments and analysis as a function of the temperature, and in this respect experiments on powders have, as compared to single crystals, the advantage of easier and less time consuming data collection. The parameter field with the variables temperature and scattering vector forming the basis in all the equations can really be investigated and the systematics of derived parameter values can be followed.

Acknowledgments

Author BG would like to thank the LNS for the support of the present study. Dr H Boysen (University of Munich) provided the software for the anharmonic analysis and is also gratefully acknowledged for many stimulating discussions. Thanks are due to M Koch and R Thut for technical assistance. This work was partly supported by the Nationaler Energie-Forschungs-Fonds, grant 478.

References

[1] Wykoff R W G 1963 *Crystal Structures* vol I (New York: Wiley–Interscience)
[2] Tubandt C 1932 *Handbuch der Experimentalphysik* vol XII/1 (Leipzig: Akademische Verlagsgesellschaft) pp 446–9
[3] Schaake H P 1969 *AFCRL Report* 69-0538 (cited in [4])
[4] Prevot B, Hennion B and Dorner B 1977 *J. Phys. C: Solid State Phys.* **10** 3999–4011
[5] Hoshino S, Fujii Y, Harada J and Axe J D 1976 *J. Phys. Soc. Japan* **41** 965–73
[6] Cooper M J, Rouse K D and Willis B T M 1968 *Acta Crystallogr.* A **24** 484–93
[7] Mair S L, Barnea Z, Cooper M J and Rouse K D 1974 *Acta Crystallogr.* A **30** 806–13
[8] Cooper M J, Rouse K D and Fuess H 1973 *Acta Crystallogr.* A **29** 49–56
[9] Bührer W and Hälg W 1977 *Electrochim. Acta* **22** 701–5

[10] Harada J, Suzuki H and Hoshino S 1976 *J. Phys. Soc. Japan* **41** 1707–15
[11] Sakata M, Hoshino S and Harada J 1974 *Acta Crystallogr.* A **30** 655–61
[12] Graneli B, Dahlborg U and Fischer P 1988 *Solid State Ion.* **28–30** 284–93
[13] Yude Y, Boysen H and Schulz H 1990 *Z. Kristallogr.* **191** 79–91
[14] Schefer J, Fischer P, Heer H, Isacson A, Koch M and Thut R 1990 *Nucl. Instrum. Methods* A **288** 477–85
[15] Bacon G E 1975 *Neutron Diffraction* 3rd edn (Oxford: Clarendon)
[16] Willis B T M and Pryor A W 1975 *Thermal Vibrations in Crystallography* (Cambridge: Cambridge University Press)
[17] Willis B T M 1969 *Acta Crystallogr.* A **25** 277–300
[18] Zucker U H and Schulz H 1982 *Acta Crystallogr.* A **38** 563–8
[19] Rietveld H M 1969 *J Appl. Crystallogr.* **2** 65–71
[20] Boysen H 1990 *Acta Crystallogr.* A **46** Supplement C-308, PS-08.03.14
[21] Boysen H 1992 *'Accuracy in Powder Diffraction II' Proc.* ed E Prince and J Stalick J (Gaithersburg: NIST) pp 165–74
[22] *Sears* V F 1992 *Neutron News* **23** 26–37
[23] Cooper M J and Rouse K D 1968 *Acta Crystallogr.* A **24** 405–10
[24] Schäfgen H P 1982 *Thesis* Abteilung für Chemie, University of Bochum
[25] Butt N M, Rouse K D and Thomas M W 1978 *Acta Crystallogr.* A **34** 759–61